Available online at www.sciencedirect.com

SciVerse ScienceDirect

Ceramics International 38 (2012) 1057–1063

CERAMICS INTERNATIONAL

www.elsevier.com/locate/ceramint

Influence of deposition parameters and annealing treatment on the properties of GZO films grown using rf magnetron sputtering

C.H. Huang [a], D.Y. Chen [b], C.Y. Hsu [a,*]

[a] Department of Mechanical Engineering, Lunghwa University of Science and Technology, Taoyuan, Taiwan, ROC
[b] Department of Mechanical Engineering, Hwa Hsia Institute of Technology, Taipei, Taiwan, ROC

Received 27 April 2011; received in revised form 14 August 2011; accepted 14 August 2011
Available online 24 August 2011

Abstract

In this study, transparent conductive films of gallium-doped zinc oxide (GZO) are deposited on soda–lime glass substrates, under varied coating conditions (rf power, sputtering pressure, substrate-to-target distance and deposition time), using radio frequency (rf) magnetron sputtering, at room temperature. The effect of the coating parameters on the structural, morphological, electrical and optical properties of GZO films was studied. This study uses a grey-based Taguchi method, to determine the parameters of the coating process for GZO films, by considering multiple performance characteristics. In the confirmation runs, with grey relational analysis, improvements of 14.1% in the deposition rate, 39.81% in electrical resistivity and 1.38% in visible range transmittance were noted. The influence of annealing treatment, in a vacuum, oxygen, and nitrogen gas atmospheres, at temperatures ranging from 130 to 190 °C, for a period of 1 h, was also investigated. GZO films annealed at 190 °C, in a vacuum, showed the lowest electrical resistivity, at 1.07×10^{-3} Ω-cm, with about 85% optical transmittance, in the visible region. It is likely that films grown at lower temperatures (190 °C) could be coated onto polymeric substrates, to produce flexible optoelectronic devices.

Keywords: GZO; Grey relational analysis; Annealing treatment; Electrical and optical properties

1. Introduction

Zinc oxide (ZnO) transparent conducting films have excellent electrical and optical properties and find uses in liquid crystal displays, gas sensors, solar cells, piezoelectric devices, various optoelectronic devices and surface acoustic wave (SAW) devices [1,2]. ZnO thin films have also found uses as a transparent conducting oxide (TCO) material, in solar cells based on Si and Cu (InGa) Se_2 [3]. The advantages of zinc oxide over ITO and SnO_2 films are its low material cost, non-toxicity, high crystallinity and stability in hydrogen plasma processes [4]. The addition of Group III metal dopants, such as Al, In and Ga, increases the electrical conductivity and transparency of ZnO films [5]. The incorporation of these elements into the ZnO lattice can stabilize the film, at high temperatures, and increase its electrical conductivity [6]. Of these dopants, Ga has several advantages, in that it is less reactive and more resistant to oxidation than Al [7]. The occurrence of defects is minimized, when ZnO is doped with Ga, since the radius of Ga^{3+} (0.062 nm) is closer to that of Zn^{2+} (0.060 nm) than that of Al^{3+} (0.053 nm) [8]. The diffraction patterns show that deposited Ga-doped ZnO films exhibit a hexagonal structure, which indicates that the Ga atoms substitute for Zn, in the hexagonal lattice [9], and Ga ions occupy the interstitial sites of ZnO, or segregate to the non-crystalline region in grain boundaries and form Ga–O bonds [10]. There are different growth techniques for ZnO films doped with Ga (GZO), but the common most fabrication techniques are sputtering [11], chemical vapor deposition [12], sol–gel techniques [13] and pulsed laser deposition [14]. This study analyzes the preparation of high quality Ga-doped zinc oxide (GZO) transparent conductive films, prepared on glass substrates, using rf magnetron sputtering, at room temperature. The influence of the coating parameters on the structural, morphological, electrical and optical properties of GZO films is also investigated.

The Taguchi method, which combines experimental design theory and the quality loss function concept, is used to design robust products and processes and has solved some confusing

* Corresponding author. Tel.: +886 282 094 845; fax: +886 282 094 845.
E-mail address: cyhsu@mail.lhu.edu.tw (C.Y. Hsu).

0272-8842/$36.00
doi:10.1016/j.ceramint.2011.08.031

Table 1
Deposition parameters for GZO films, factors and levels.

Substrate	Soda–lime; thickness 1 mm
Target	97 wt.% ZnO, 3 wt.% Ga_2O_3; 99.995% purity
Gas	Argon (99.995%)
Base pressure	6.67×10^{-4} Pa
Substrate rotate vertical axis	10 rpm
Substrate temperature	Room temperature

Symbol	Process parameter	Level 1	Level 2	Level 3
A	rf power (W)	50	100	150
B	Sputtering pressure (Pa)	0.5	1	1.5
C	Substrate-to-target distance (cm)	8.5	9.5	10.5
D	Deposition time (min)	30	60	90

Table 2
L_9 (3^4) orthogonal array, with four columns and nine rows.

Experiment no.	Process parameter			
	A	B	C	D
1	1	1	1	1
2	1	2	2	2
3	1	3	3	3
4	2	1	2	3
5	2	2	3	1
6	2	3	1	2
7	3	1	3	2
8	3	2	1	3
9	3	3	2	1

problems in manufacturing [15]. This experiment uses four influential deposition parameters – rf power (A), sputtering pressure (B), substrate-to-target distance (C) and deposit time (D) – each of which is assigned high, medium and low levels, as shown in Table 1. In order to optimize the design of the deposition process for GZO films, this study uses a Taguchi L_9 (3^4) orthogonal array, with four columns and nine rows, as shown in Table 2. Then, based on grey relational analysis, optimization of the coating process parameters, with multiple qualities, for GZO films, is achieved [16]. In addition, there was also an investigation of the influence of annealing treatment, in a vacuum, oxygen and nitrogen gas atmospheres, at temperatures ranging from 130 to 190 °C, for a period of 1 h, on properties of GZO films.

2. Experimental details

GZO transparent conducting films were deposited on glass substrates, under various coating conditions, using rf magnetron sputtering, at room temperature, with a base pressure of 6.67×10^{-4} Pa. The commercially available hot-pressed and sintered target GZO (97 wt.% ZnO, 3 wt.% Ga_2O_3; 99.995% purity, Elecmat, USA) had a diameter of 50.8 mm and a thickness of 6 mm. The amount of Ga_2O_3 dopant in the ZnO powder varied, from 2 to 5% [16]. Ga_2O_3 of about 3 wt.% was chosen for this study. Before deposition, the glass substrates were ultrasonically cleaned in acetone, rinsed in deionized water and blow-dried with nitrogen. The magnetron sputtering system was microprocessor controlled.

2.1. Analysis of variance (ANOVA)

An analysis of variance (ANOVA) was performed, to evaluate the coating parameters that were statistically significant. Using the signal-to-noise (*S/N*) ratio and ANOVA analyses, the optimal combination of process parameters can be predicted [17]. A confirmation experiment was then conducted, to verify the optimal process parameters, obtained. An ANOVA and an *F*-test were used to analyze the experimental data:

$$S_m = \frac{\left(\sum \eta_i^2\right)}{9}, \qquad S_T = \sum \eta_i^2 - S_m \tag{1}$$

$$S_A = \frac{\left(\sum \eta_{Ai}^2\right)^2}{N} - S_m, \qquad S_E = S_T - \sum S_A \tag{2}$$

$$V_A = \frac{S_A}{f_A}, \qquad F_{Ao} = \frac{V_A}{V_E} \tag{3}$$

where S_T is the sum of squares, due to the total variation, S_m is the sum of squares, due to the means, S_A is the sum of squares, due to parameter A (A represents rf power, sputtering pressure, substrate-to-target, and deposit time, respectively), S_g is the sum of squares due to error, η_i is the η value of each experiment ($i = 1 \ldots 9$), η_{Ai} is the sum of the ith level of parameter A ($i = 1, 2, 3$), N is the repeating number of each level of parameter A, f_A is the degree of freedom of parameter A, V_A is the variance of parameter A and F_{Ao} is the F-test value for parameter A.

2.2. Grey relational analysis

Grey relational analysis can be used to effectively solve complicated interrelationships between multiple performance characteristics. The grey relational coefficient is [18]:

$$r(x_o(k), x_i(k)) = \frac{\min_i \min_k |x_0(k) - x_i(k)| + \zeta \max_i \max_k |x_0(k) - x_i(k)|}{|x_0(k) - x_i(k)| + \zeta \max_i \max_k |x_0(k) - x_i(k)|} \tag{4}$$

where $x_i(k)$ is the normalized value of the kth performance characteristic, in the ith experiment, and ζ is the distinguishing coefficient ($\zeta \in [0,1]$). The value of ζ can be adjusted, according to actual system requirements. The coating parameters are of equal weighting, in this study, and therefore ζ is 0.5.

The grey relational grade is a weighting-sum of the grey relational coefficient. It is defined as [18]:

$$r(x_0, x_i) = \frac{1}{n} \sum_{k=1}^{n} r(r_0(k), x_i(k)) \tag{5}$$

where n is the number of performance characteristics.

Grey relational analysis, based on the grey system theory, can be used to effectively solve complicated interrelationships between multiple performance characteristics [19]. For grey

relational analysis, the experimental results of deposition rate, electrical resistivity and transmittance are first normalized, in the range between 0 and 1, which is called grey relational generating. Using grey relational analysis [18] and statistical analysis of variance (ANOVA), the optimal combination of GZO deposition parameters can be predicted [11].

3. Results and discussion

Table 3 shows the ANOVA results for the deposition rate of GZO; the most important variable affecting the deposition rate factor is the rf power ($P = 83.40\%$). With a higher rf power, the sputtered species has a higher energy, which contributes to film growth [20]. Additionally, the substrate-to-target distance also affects the deposition rate, with a contribution ratio of 13.58%. The growth rate increases, as the substrate-to-target distance decreases [21].

Table 4 lists the ANOVA results for GZO electrical resistivity. It is evident that rf power and sputtering pressure are the process parameters that significantly affect GZO electrical resistivity. Fig. 1 shows the *S/N* response graph for the electrical resistivity of GZO. It shows that a higher rf power can causes a lower electrical resistivity. With higher rf power, the crystalline quality is enhanced [22], which leads to an increase in conductivity, due to an increase in carrier concentration and Hall mobility, and reduces the electrical resistivity of GZO films. Fig. 1 shows that resistivity decreases, as sputtering pressure is increased. This is in agreement with the results of Lin et al. [23], in that XRD patterns indicate that the intensity of the (0 0 2) diffraction peak becomes stronger, as sputtering pressure is increased, so the film crystalline quality is improved, when sputtering pressure is increased.

Table 5 shows the ANOVA results for GZO optical transmittance. It shows that the substrate-to-target distance most significantly affects the transmittance, with a contribution ratio of about 47.44%, followed by rf power, with a contribution of 32.25%. The *S/N* response graph, in Fig. 2, shows that the optical transmittance increases, as the substrate-to-target distance is decreased. Higher transmittance is also obtained, when rf power is lower.

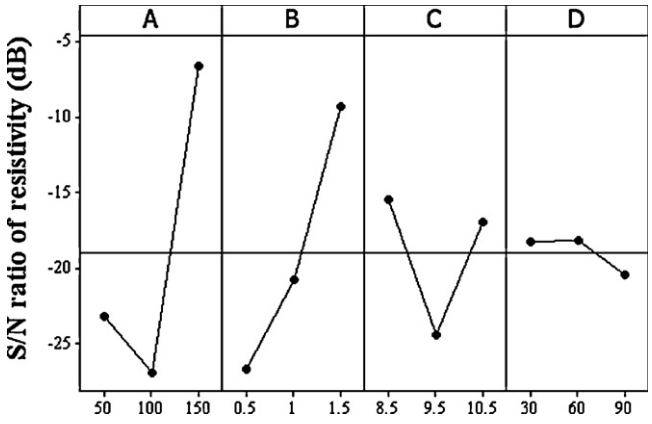

Fig. 1. *S/N* response graph, for GZO electrical resistivity.

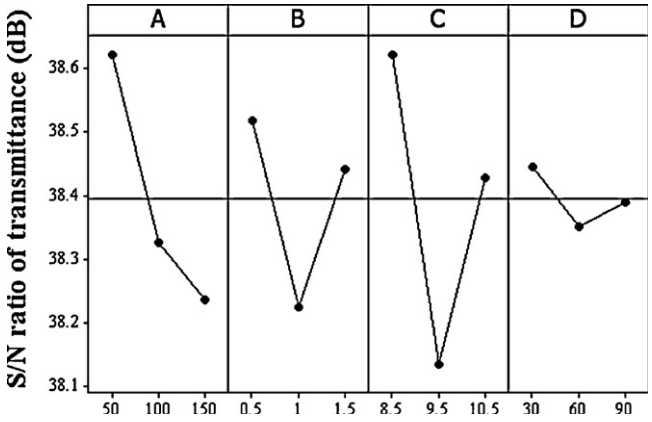

Fig. 2. *S/N* response graph, for GZO optical transmittance.

Table 3
ANOVA results, for GZO deposition rate.

Process parameter	Degree of freedom (F)	Sum of square (S)	Variance (V)	Contribution (P %)
A	2	138.33	69.16	83.40
B	2	3.45	1.73	2.08
C	2	22.52	11.26	13.58
D	2	1.56	0.78	0.94
Total	8	165.87		100

Table 4
ANOVA results, for GZO electrical resistivity.

Process parameter	Degree of freedom (F)	Sum of square (S)	Variance (V)	Contribution (P %)
A	2	701.09	350.55	53.18
B	2	469.52	234.76	35.62
C	2	137.67	68.84	10.44
D	2	10.01	5.01	0.76
Total	8	1318.29		100

Table 5
ANOVA results, for GZO optical transmittance.

Process parameter	Degree of freedom (F)	Sum of square (S)	Variance (V)	Contribution (P %)
A	2	0.24	0.12	32.25
B	2	0.14	0.07	18.54
C	2	0.36	0.18	47.44
D	2	0.01	0.006	1.77
Total	8	0.76		100

The X-ray diffraction patterns for the GZO films no's 1–9, of the L_9 orthogonal array, are presented in Fig. 3. It is apparent that, for all of the films, only the (0 0 2) diffraction peaks located at $2\theta \sim 34.4^\circ$ are observed, showing that the GZO films have hexagonal ZnO Wurtzite structure, with a preferential orientation along the c-axis, perpendicular to the substrate surface. For GZO film no. 8 ($A_3B_2C_1D_3$), in the orthogonal array, the diffraction peaks are sharper and more intense. This is due to an increase in the crystallite size and an improvement in the crystallinity of the films.

Based on Eqs. (4) and (5), the grey relational grade for each experiment, using the L_9 orthogonal array, is shown in Table 6. A higher grey relational grade indicates that the corresponding experimental result is closer to the ideally normalized value and demonstrates the multiple performance characteristics for deposition GZO films, as predicted by the orthogonal array ($A_3B_2C_1D_3$) and grey theory ($A_3B_3C_1D_1$). Table 7 shows the multiple performance characteristics for the orthogonal array and the grey relational optimal predicted deposition process parameters, for GZO films. From Table 7, comparing the grey theory prediction ($A_3B_3C_1D_1$) with the orthogonal array process parameters ($A_3B_2C_1D_3$), it is seen that the GZO deposition rate increases, from 12.07 to 13.77 nm/min, electrical resistivity is reduced, from 2.11 to 1.27×10^{-3} Ω-cm, and optical transmittance is slightly improved, from 82.14 to 83.27%. The experimental conditions ($A_3B_3C_1D_1$) were tested, three times. For the confirmation run, the deposition rate was 13.56 nm/min, electrical resistivity was 1.28×10^{-3} Ω-cm and optical transmittance was 83.89%. These results are consistent with the 3D AFM images of the GZO films, seen in Fig. 4. It is evident that, using the grey theory prediction, the GZO films have smoother surfaces and larger crystallite size (see Fig. 4b), with lower electrical resistivity and higher optical transmittance.

Fig. 5 shows the XRD patterns of the GZO thin films deposited using the grey theory prediction ($A_3B_3C_1D_1$) and annealed in a vacuum, oxygen and nitrogen atmospheres, at temperatures ranging from 130 to 190 °C, for a period of 1 h. The results indicate that all of the films show a good c-axis orientation, corresponding to vertical growth, with respect to

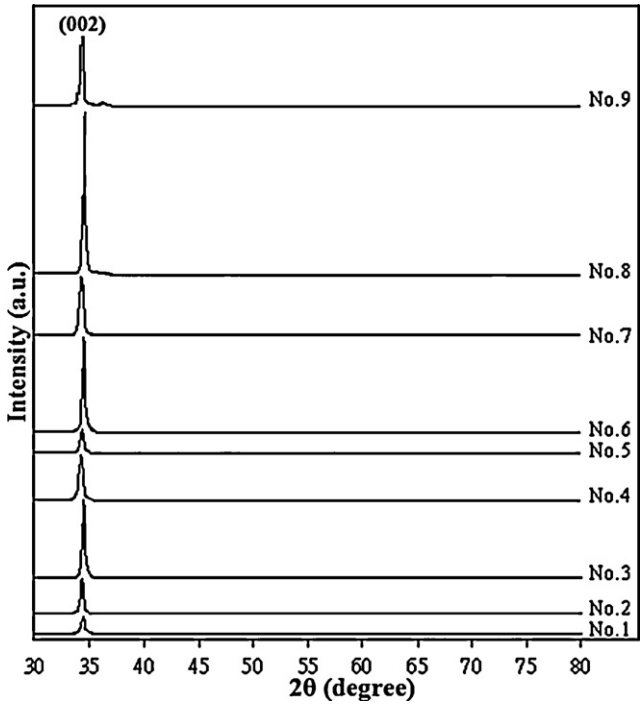

Fig. 3. XRD patterns of GZO films grown on glass, for no's 1–9, of the L_9. orthogonal array.

Table 6
Grey relational grade and orders.

Experiment no.	Process parameter				Grey relational grade	Order
	A	B	C	D		
1	1	1	1	1	0.7069	2
2	1	2	2	2	0.4507	8
3	1	3	3	3	0.6219	5
4	2	1	2	3	0.3700	9
5	2	2	3	1	0.5256	7
6	2	3	1	2	0.6596	4
7	3	1	3	2	0.6660	3
8	3	2	1	3	0.7918	1
9	3	3	2	1	0.6188	6

Table 7
Multiple performance characteristics, with orthogonal array and grey relational optimal predictions for deposition process parameters.

	Orthogonal array	Grey theory prediction design	Improvement rate (%)
Level	$A_3B_2C_1D_3$	$A_3B_3C_1D_1$	
Deposition rate (nm/min)	12.07	13.77	14.1
Resistivity (10^{-3} Ω cm)	2.11	1.27	39.81
Transmittance (%)	82.14	83.27	1.38

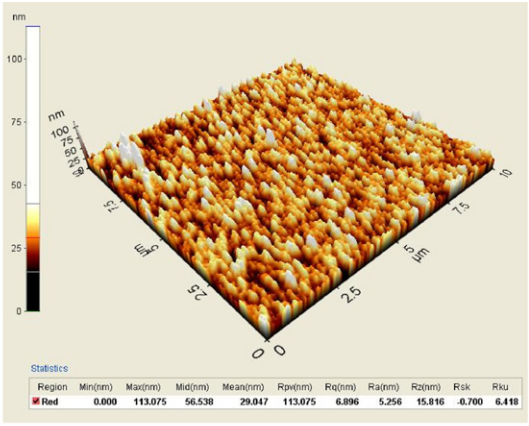

(a) Surface roughness (Ra)= 5.26 nm, thickness=1086 nm, grain size=25.35 nm

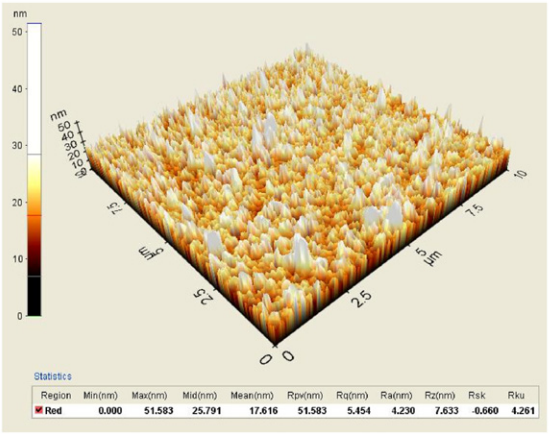

(b) Surface roughness (Ra)= 4.23 nm, thickness=410 nm, grain size=29.62 nm

Fig. 4. 3D AFM images of GZO films: (a) orthogonal array parameters, (b) grey theory prediction design. (a) Surface roughness (Ra) = 5.26 nm, thickness = 1086 nm, grain size = 25.35 nm (b) surface roughness (Ra) = 4.23 nm, thickness = 410 nm, grain size = 29.62 nm.

the substrate. There is no significant change in the orientation of films annealed in different atmospheres. The intensity of the X-ray peaks increases, after annealing leads to an improvement in the crystallinity of the films. A comparison of the as-deposited films with those that were annealed shows a steady decrease in full width at half maximum (FWHM), in the case of vacuum annealing. The as-deposited GZO thin film has a FWHM value of 0.281, while the GZO thin film annealed at 190 °C, in a vacuum, for 1 h, has a value of 0.261. Scherrer's equation is used to calculate the crystallite size. Fig. 6 shows the crystallite size of the GZO films, as a function of annealing temperature, in different atmospheres. The crystallite size of the GZO films is increased, by annealing in a vacuum atmosphere, regardless of annealing temperature.

Fig. 7 shows the electrical resistivity of GZO films, as a function of annealing temperature, in various atmospheres. The results show that the electrical properties are strongly dependent on the type of gas. It is apparent that the electrical resistivity of the GZO films annealed in a vacuum, or oxygen

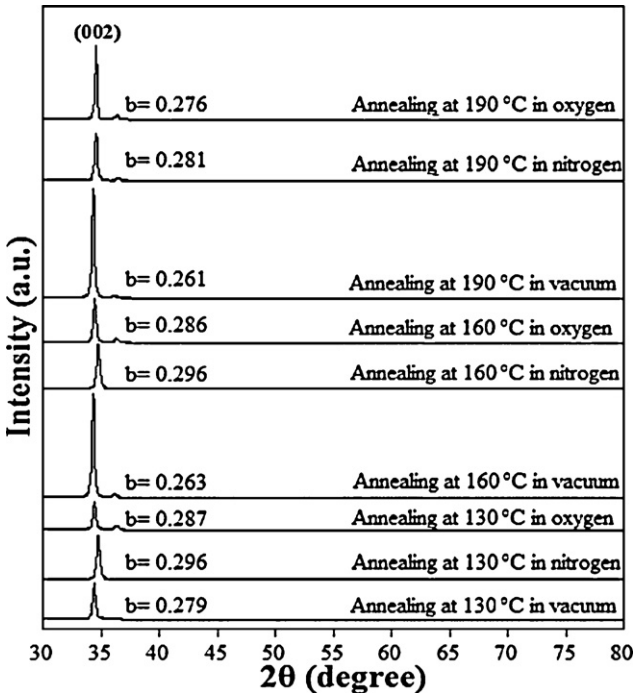

Fig. 5. X-ray diffraction patterns for GZO films annealed at temperatures ranging from 130 to 190 °C, for 1 h, in a vacuum, oxygen and nitrogen atmospheres (b: full width at half maximum, FWHM).

environment is lower than that for as-deposited samples. However, GZO films annealed in a nitrogen atmosphere have the highest value of resistivity. The transmission spectra of the GZO films, as a function of annealing temperature, in different atmospheres, are shown in Fig. 8. The average transmittance of the GZO films, in the visible region (500 ~ 800 nm), before annealing, was 83.27%, while after annealing at 190 °C, in a vacuum, the average transmittances were 85.13%. After annealing at 190 °C, in oxygen and nitrogen environments, the average transmittances were 82.81%, and 82.45%, respectively.

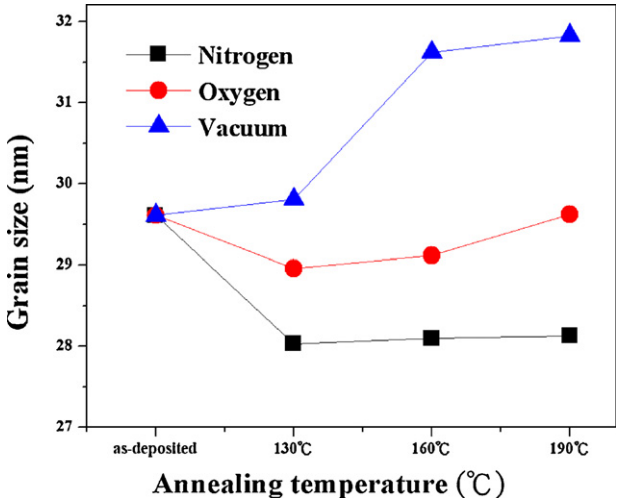

Fig. 6. The crystallite size of GZO films, as a function of annealing temperature, in different atmospheres.

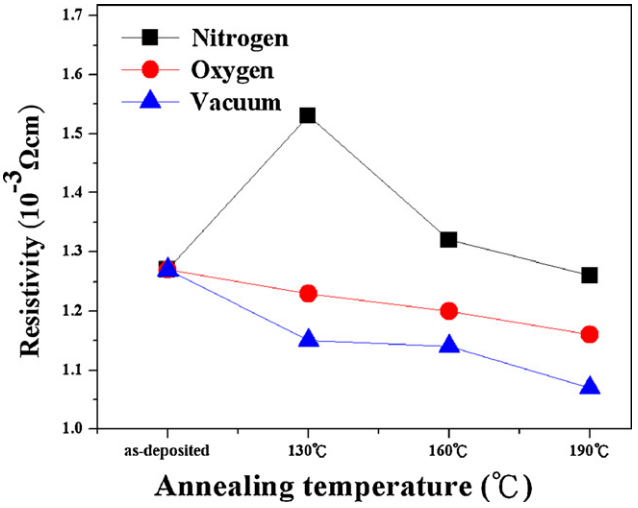

Fig. 7. The electrical resistivity of GZO films, as a function of annealing temperature, in different atmospheres.

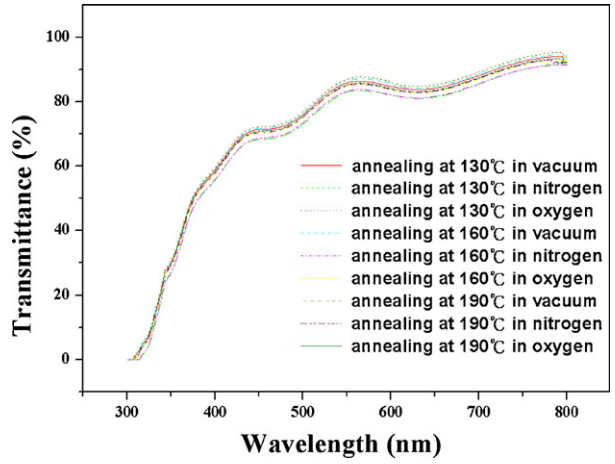

Fig. 8. The optical transmittance of GZO films, as a function of annealing temperature, in different atmospheres.

4. Conclusions

Transparent conductive films of gallium-doped zinc oxide (GZO) were fabricated on a soda–lime glass substrate, using rf magnetron sputtering and low substrate temperatures. An L_9 (3^4) orthogonal array was used, with grey relational analysis, to optimize the GZO films, using multiple performance characteristics. The effect of various deposition conditions, on structure and optoelectronic properties of the GZO films, was also investigated. Using the grey theory prediction ($A_3B_3C_1D_1$), the crystallinity of the GZO film increased, the deposition rate increased, from 12.07 to 13.77 nm/min, electrical resistivity decreased, from 2.11×10^{-3} to 1.27×10^{-3} Ω-cm, and optical transmittance increased, slightly, from 82.14 to 83.27%. It was also seen that annealing at a higher temperature (190 °C) causes a decrease in electrical resistivity more effectively than annealing at a lower temperature (130 °C). The lowest electrical resistivity of 1.07×10^{-3} Ω-cm, and the highest optical transmittance of 85.13% were noted, for annealing at 190 °C, in a vacuum atmosphere.

References

[1] T. Minami, T. Yamamoto, T. Miyata, Highly transparent and conductive rare earth-doped ZnO thin films prepared by magnetron sputtering, Thin Solid Films 366 (2000) 63–68.
[2] A. Kassis, M. Saad, Fill factor losses in ZnO/CdS/$CuGaSe_2$ single-crystal solar cells, Solar Energy Materials & Solar Cells 80 (2003) 491–499.
[3] N.F. Cooray, K. Kushiya, A. Fujimaki, I. Sugiyama, T. Miura, D. Okumura, M. Sato, M. Ooshita, O. Yamase, Large area ZnO films optimized for graded band-gap Cu(InGa)Se_2-based thin-film mini-modules, Solar Energy Materials & Solar Cells 49 (1997) 291–297.
[4] M. Miyazaki, K. Sato, A. Mitsui, H. Nishimura, Properties of Ga-doped ZnO films, Journal of Non-Crystalline Solids 218 (1997) 323–328.
[5] R.K. Shukla, A. Srivastava, A. Srivastava, K.C. Dubey, Growth of transparent conducting nanocrystalline Al doped ZnO thin films by pulsed laser deposition, Journal of Crystal Growth 294 (2006) 427–431.
[6] H. Ǵomez, M. de la, L. Olvera, Ga-doped ZnO thin films: effect of deposition temperature, dopant concentration, and vacuum-thermal treatment on the electrical, optical, structural and morphological properties, Materials Science and Engineering B 134 (2006) 20–26.
[7] V. Assuncao, E. Fortunato, A. Marques, H. Aguas, I. Ferreira, M.E.V. Costa, R. Martins, Influence of the deposition pressure on the properties of transparent and conductive ZnO:Ga thin-film produced by r.f. sputtering at room temperature, Thin Solid Films 427 (2003) 401–405.
[8] K. Yim, H.W. Kim, C. Lee, Effects of annealing on structure, resistivity and transmittance of Ga doped ZnO films, Materials Science and Technology 23 (2007) 108–112.
[9] X.Y Li, H.J. Li, Z.J. Wang, H. Xia, Z.Y. Xiong, J.X. Wang, B.C. Yang, Effect of substrate temperature on the structural and optical properties of ZnO and Al-doped ZnO thin films prepared by dc magnetron sputtering, Optics Communications 282 (2009) 247–252.
[10] Q.B. Ma, Z.Z. Ye, H.P. He, S.H. Hu, J.R. Wang, L.P. Zhu, Y.Z. Zhang, B.H. Zhao, Structural, electrical, and optical properties of transparent conductive ZnO:Ga films prepared by DC reactive magnetron sputtering, Journal of Crystal Growth 304 (2007) 64–68.
[11] D.Y Chen, C.Y. Hsu, Growth of Ga-doped ZnO films with ZnO buffer layer by sputtering at room temperature, Superlattices and Microstructures 44 (2008) 742–753.
[12] K. Haga, T. Suzuki, Y. Kashiwaba, H. Watanabe, B.P. Zhang, Y. Segawa, High-quality ZnO films prepared on Si wafers by low-pressure MO-CVD, Thin Solid Films 433 (1–2) (2003) 131–134.
[13] K.Y. Cheong, N. Muti, S.R. Ramanan, Electrical and optical studies of ZnO:Ga thin films fabricated via the sol–gel technique, Thin Solid Films 410 (2002) 142–146.
[14] G.A. Hirata, J. McKittrick, T. Cheeks, J.M. Siqueiros, J.A. Diaz, O. Contreras, O.A. Lopez, Synthesis and optelectronic characterization of gallium doped zinc oxide transparent electrodes, Thin Solid Films 288 (1996) 29–31.
[15] C.Y. Nian, W.H. Yang, Y.S. Tarng, Optimization of turning operations with multiple performance characteristics, Journal of Materials Processing Technology 95 (1999) 90–96.
[16] C.Y. Hsu, C.H. Tsang, Effects of ZnO buffer layer on the optoelectronic performances of GZO films, Solar Energy Materials & Solar Cells 92 (2008) 530–536.
[17] M. Nalbant, H. Gokkaya, G. Sur, Application of Taguchi method in the optimization of cutting parameters for surface roughness in turning, Materials and Design 28 (2007) 13791385.
[18] J.L. Deng, Introduction to grey system, Journal of Grey System 1 (1) (1989) 1.
[19] Y.S. Tarng, S.C. Juang, C.H. Chang, The use of grey-based Taguchi methods to determine submerged arc welding process parameters in hardfacing, Journal of Materials Processing Technology 128 (2002) 1–6.

[20] X. Yu, J. Ma, F. Ji, Y. Wang, X. Zhang, C. Cheng, H. Ma, Effects of sputtering power on the properties of ZnO:Ga films deposited by r.f. magnetron sputtering at low temperature, Journal of Crystal Growth 274 (2005) 474–479.

[21] V. Assuncao, E. Fortunato, A. Marques, A. Goncalves, I. Ferreira, H. Aguas, R. Martins, Growth of ZnO:Ga thin films at room temperature on polymeric substrates: thickness dependence, Thin Solid Films 442 (2003) 121–126.

[22] E. Fortunato, P. Nunes, D. Costa, D. Brida, I. Ferreira, R. Martins, Characterization of aluminium doped zinc oxide thin films deposited on polymeric substrates, Vacuum 64 (2002) 233–236.

[23] Y.C. Lin, M.Z. Chen, C.C. Kuo, W.T. Yen, Electrical and optical properties of ZnO:Al film prepared on polyethersulfone substrate by RF magnetron sputtering, Colloids and Surfaces A: Physicochemical and Engineering Aspects 337 (2009) 52–56.